Published in IET Nanobiotechnology
Received on 13th November 2012
Revised on 14th March 2013
Accepted on 22nd March 2013
doi: 10.1049/iet-nbt.2012.0041

Special Issue: Recent Advances in Biosynthesis of Nanoparticles and their Applications

ISSN 1751-8741

Biological synthesis of metallic nanoparticles using algae

Laura Castro, María Luisa Blázquez, Jesus Angel Muñoz, Felisa González, Antonio Ballester

Department of Material Science and Metallurgic Engineering, Faculty of Chemistry, Complutense University of Madrid, Avda. Complutense s/n, 28040 Madrid, Spain
E-mail: mlblazquez@quim.ucm.es

Abstract: The increasing demand and limited natural resources of noble metals make its recovery from dilute industrial wastes attractive, especially when using environmentally friendly methods. Nowadays, the high impact that nanotechnology is having in both science and society offers new research possibilities. Gold and silver nanoparticles were biosynthesised by a simple method using different algae as reducing agent. The authors explored the application of dead algae in an eco-friendly procedure. The nanoparticle formation was followed by UV–vis absorption spectroscopy and transmission electron microscopy. The functional groups involved in the bioreduction were studied by Fourier transform infrared spectroscopy.

1 Introduction

Metal nanoparticles have a great scientific interest because of their unique optoelectronic and physicochemical properties with applications in diverse areas such as electronics [1], catalysis [2], drug delivery [3] or sensing [4]. The excellent properties of some materials strongly depend on crystallographic and morphological characteristics. In consequence, scientists have focused the research on the synthesis of nanoparticles with a controlled shape and size. A variety of shapes such as nanorods [5], nanowires [6], nanocubes [7] and nanodisks [8] have been obtained using several chemical and physical methods. However, these methods employ toxic chemicals as reducing agents, organic solvents or non-biodegradable stabilising agents.

Moreover, recycling noble metals is both economically and environmentally interesting because of their high global market prices, finite ore deposits and excessive and harmful mining processes. Nowadays, there is a necessity to search for alternative pyrometallurgical and hydrometallurgical recycling processes that require less energy and cause less pollution. Currently, biosynthesis of nanoparticles has attracted scientists' attention because of the necessity to develop new clean, cost-effective and efficient synthesis techniques.

Even though many biotechnological applications such as the remediation of toxic metals employ organisms such as bacteria [9] and fungi [10], such organisms have been described as possible eco-friendly nanofactories [11, 12]). Processes devised by nature for the synthesis of inorganic materials on nano- and micro-length scales have contributed to the development of a relatively new and largely unexplored area of research based on the use of different organisms in the biosynthesis of nanomaterials [13]. Biosynthesis of metal nanoparticles has been reported using bacteria, yeasts, actinomycetes, fungi and plants [14, 15].

Algae are eukaryotic aquatic oxygenic photoautotrophs, and some of them are able to accumulate various heavy metals. However, there are very few reports about biological synthesis of noble metal nanoparticles using algae.

The dried alga *Chlorella vulgaris*, a single-celled green alga, was found to have strong binding ability towards tetrachloroaurate ions to form algal-bound gold, which was subsequently reduced to Au(0). Approximately 88% of algal-bound gold attained metallic state and the crystals of gold were accumulated in the inner and outer parts of cell surfaces with tetrahedral, decahedral and icosahedral structures [16].

Spirulina platensis is an edible blue–green alga and the dried alga was used for the extracellular synthesis of gold, silver and Au/Ag bimetallic nanoparticles [17]. More recently, Singaravelu *et al.* [18] and Rajasulochana *et al.* [19] reported the synthesis of extracellular metal bionanoparticles using *Sargassum wightii* and *Kappaphycus alvarezii*, respectively. Also, Senapati *et al.* [20] reported the intracellular production of gold nanoparticles using *Tetraselmis kochinensis*. Moreover, our group previously reported on the bioreduction of Au(III)–Au(0) using biomass of the brown alga *Fucus vesiculosus* [21].

In this work, biosynthesis of gold nanoparticles has been investigated using aqueous chloroaurate ions and dead algae as a clean technology to recover gold from dilute solutions. This procedure presents the remarkable advantage of using algae, an unlimited source of raw material. To our knowledge, biosynthesis of metal nanostructures using algae as reducing agents has not been frequently reported. The objectives of this study were to investigate a cheap and clean method for nanoparticles formation using algae as reducing agent and to determine the optimal conditions for the synthesis and the control of the particle morphology. The achievement of this work was the possibility to control

the shape by means of a biological procedure changing variables such as the type of biomass (*Chondrus crispus* and *Spyrogira insignis*) and solution pH.

2 Experimental section

2.1 Materials

All chemical reagents including chloroauric acid ($HAuCl_4$), silver nitrate ($AgNO_3$), sodium hydroxide flakes and hydrochloric acid (37%) were obtained from Panreac and used as received.

2.2 Algae preparation

C. crispus was provided by Algamar plant in Redondela (Pontevedra, Spain). The red alga was collected in Spring 2003. *S. insignis*, a freshwater green alga, was sampled in Valmayor reservoir (Madrid, Spain) in summer 2001.

The algae were washed with deionised water and then dried in a stove at 60°C and ground with an agate mortar. In experiments, biomass size lower than 0.5 mm was used.

2.3 Synthesis of gold nanoparticles

Different initial pH values (2–10) of 0.5×10^{-3} M aqueous $HAuCl_4$ solutions were prepared. The experimental method consisted in mixing 50 ml of aqueous solution of tetrachloroaurate with the different types of algae and stirring at room temperature. For the synthesis of gold nanoparticles, 0.25 g of alga was added to solutions. Several samples were collected at different times of reaction for analysis. The biomass was removed from the reaction mixture by filtration using nylon membrane filters 0.2 μm from Whatman.

2.4 Synthesis of silver nanoparticles

Different initial pH values (2–10) of 0.5×10^{-3} M aqueous $AgNO_3$ solutions were prepared. The experimental method consisted in mixing 50 ml of aqueous solution of tetrachloroaurate with the green alga *S. insignis* and stirring at room temperature. For the synthesis of silver nanoparticles, 0.25 g of alga was added to solutions. Several samples were collected at different times of reaction for analysis. The biomass was removed from the reaction mixture by filtration using nylon membrane filters 0.2 μm from Whatman.

2.5 UV–vis absorbance spectroscopy studies

The UV–vis spectra for the reaction solution of gold nanoparticles were carried out on a Libra S11 single beam spectrophotometer operated at a resolution of 5 nm with quartz cells. Blanks for each of the sample sets were deionised water.

2.6 Transmission electron microscopy (TEM) measurements

TEM samples of the gold nanoparticles synthesised using the algae were prepared by placing drops of the product solution onto carbon-coated copper grids and allowing the solvent to evaporate. TEM measurements were performed on a JEOL model JEM-2000FX instrument operated at an accelerating voltage of 200 kV.

2.7 Scanning electron microscope (SEM)–energy-dispersive X-ray spectroscopy (EDS) study

S. insignis after reduction process was coated with a thin layer of graphite and examined in a SEM (JEOL JSM-6400) with an energy-dispersive elemental analyser. The chemical composition of the products was determined by EDS using a JEOL model JEM-2000FX instrument.

2.8 Fourier transform infrared (FTIR) measurements

For FTIR spectra analysis, the biomasses and nanoparticles synthesised were made in a KBr pellet and the spectra were recorded with a Nicolet Magna 750 in the region of 500–4000 cm^{-1} at a resolution of 4 cm^{-1}. The pellet was made with 0.5–3 mg of sample and approximately 250 mg of KBr.

3 Results and discussion

Nanoparticles formation using the red alga *C. crispus* and the green alga *S. insignis* under different experimental conditions was studied in the present research. The rate of nanoparticle formation and therefore the size of the nanoparticles can be manipulated by controlling different parameters [22]. Efforts have also been made to manipulate the shape and size of gold nanoparticles produced extracellularly through altering key parameters [23, 24]. In an attempt to control the size and shape of the metallic nanoparticles, the effect of parameters such as pH or time exposed to metallic precursors using different biomasses was investigated.

3.1 Use of red alga C. crispus

C. crispus is small purplish-red seaweed (up to 22 cm long) found on rocky shores and in pools. Several authors [25] have reported that the cell wall polysaccharide carrageenan can bind heavy metals. They suggested that levels of sulphation in carrageenans may account for their different abilities to bind heavy metals. This red alga was tested because of well known ability of sulphur to cap and stabilise gold nanoparticles.

3.1.1 Effect of initial pH on the biosynthesis of gold nanoparticles and UV–vis study: In this study, the influence of the pH solutions was analysed and *C. crispus* was added to aqueous $HAuCl_4$ solutions with pH values from 2 to 10. The colour changed from pale yellow to dark blue or pink (Fig. 1*a*) after reaction with biomass. This change of colour indicated the reduction of the aqueous chloroaurate ions during the exposure to the seaweed and the formation of gold nanoparticles. The different colour of the solution as a function of pH shows that the shape and size of the nanoparticles produced using this technique can be controlled through pH adjustment. The morphology of the nanoparticles obtained at different initial pH values was analysed using UV–vis spectroscopy.

It is well known that the differences in UV–vis absorption spectra and colour of solution could be dependent on different surrounding media and size, shape and structure of the gold nanoparticles. As a consequence of these changes in the morphology of nanoparticles, some differences could be observed in the UV–vis absorption spectra recorded from aqueous solutions at different initial pH values after reaction (Figs. 1*b–d*). At pH 2 and 4, a surface plasmon resonance (SPR) band absorption peak appears centred at

doi: 10.1049/iet-nbt.2012.0041

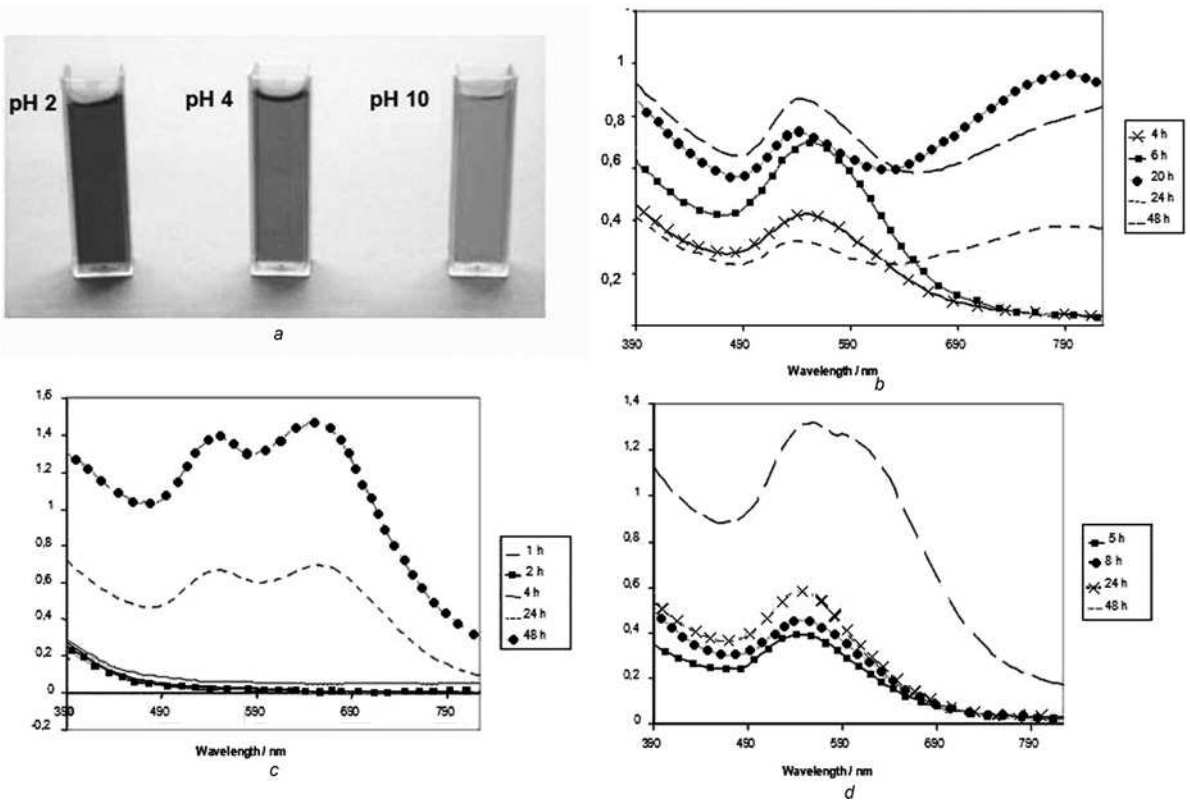

Fig. 1 *Effect of initial pH on the biosynthesis of gold nanoparticles and UV–vis study*

a Colour changes of gold nanoparticle solutions at different pH values. UV–vis spectra of gold nanoparticles prepared using *C. crispus* at different reaction time
b pH 2
c pH 4
d pH 10

approximately 540 nm, which is characteristic of gold nanoparticles. At a longer wavelength, a second band related to aggregates of spherical nanoparticles [26] or anisotropic nanostructures [27] is shown. The second band appears at 800 nm at pH 2 and at 655 at pH 4. The relative intensity and position of the second band occurs in the near IR region and is a function of the initial pH value.

At pH 10, the spectrum exhibits two resonance wavelengths practically overlapped at approximately 560 nm associated to the formation of the sphere-shaped nanoparticles, where all their electronic oscillations are equivalent.

The initial pH of the chloroaurate solutions was found to be an important parameter affecting gold nanoparticle synthesis using the red alga. Variations in pH did have an impact on the shape and size of the gold nanoparticles obtained.

In general, the reduction reaction of metallic ions is sensitive to the solution's pH as it may affect the product's morphology, but the pH had also a strong influence in the yield of the process. The yield was determined measuring the gold ions concentration in solution by flame atomic absorption spectroscopy (FAAS).The yield at pH 2 was approximately 70%. However, when the pH increased to 4, 7 and 10, the yield of the process was over 55%. At higher pH, there may be competition from the hydroxide ion for the gold ion. In fact, hydroxide is a strong complexing agent of gold ion ($\log K_3 = 38.6$) and could interfere on the reducing and capping ability of molecules present in the alga.

3.1.2 TEM characterisation of gold nanoparticles:

The morphology of the gold nanoparticles was observed by TEM. Fig. 2 shows representative TEM images of the nanoparticles synthesised using *C. crispus* at different pH values. TEM observations revealed that gold nanoparticles formed at the acidic medium were polygonal mainly triangular and hexagonal (Figs. 2*a* and *b*). The edge length of these particles can reach more than 200 nm at pH 2. When the pH was increased to 4, the size underwent a decrease, but polyhedral shape of the nanoparticles remained and spherical nanoparticles (~30 nm) were formed. An increase of initial solution pH favoured the formation of spherical nanoparticles and the presence of two different sizes, some particles presented a diameter about 50 nm and others about 30 nm, would explain the two overlapped bands in UV–vis spectrum.

The synthesis of gold nanotriangles under acidic conditions could be produced by slow reduction and the slow crystallisation leads to the formation of stable multiply twinned particles, which evolve into gold nanotriangles because of the shape-directing effect of the constituents of the red seaweed. Moreover, the difference in the growth rates of the various crystallographic planes could lead to changes in morphology of the nanoparticles [28]. We found possible to control the nanoparticles shape through the dependence on solutions pH producing polygonal nanoparticles at acidic media and nanospheres in basic conditions.

The nature of the nanoparticles was confirmed as elemental Au using EDS as shown in Fig. 3. Signals from Cl, Na or Ca are because of the emission of salts in the marine alga and Cu signals are because of the copper grids to hold the samples.

3.1.3 Functional groups involved in the biosynthesis of gold nanoparticles:

The nature of the biomolecules

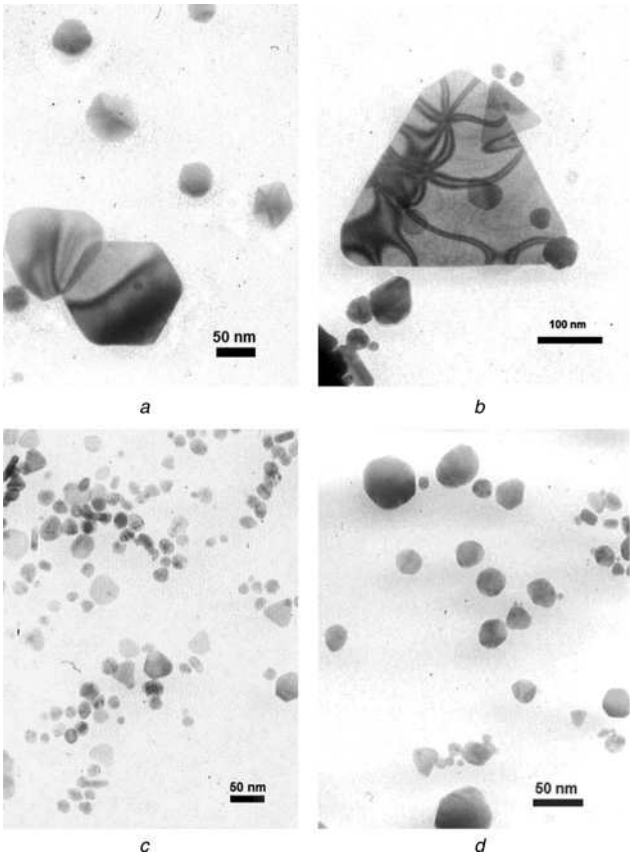

Fig. 2 *TEM images of gold nanostructures synthesised using C. crispus at different initial pH values*

a Detail of hexagonal nanoparticles obtained at pH 2
b Detail of a nanotriangle obtained at pH 2
c pH 4
d pH 10

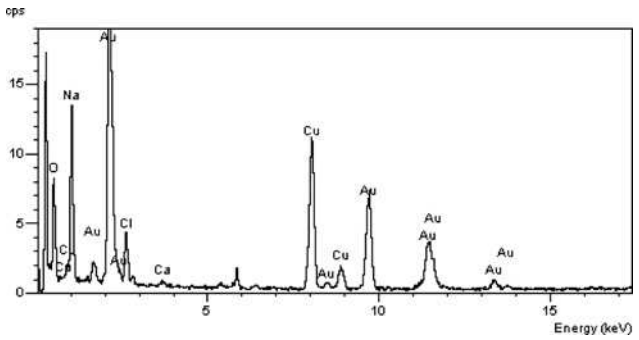

Fig. 3 *EDS of gold nanoparticles synthesised using the red seaweed C. crispus*

involved in the reduction and formation of gold nanoparticles was studied by FTIR analysis of the biomass before and after reduction of the nanoparticles (Fig. 4*a*). The spectra of the biomass before and after gold reduction show the same bands. The intense broad absorbance at approximately 3400 cm^{-1} is attributed to the O–H stretching vibration modes of hydroxyl functional group in alcohols and N–H stretching vibrations in amides and amines. The absorption peak at 2930 cm^{-1} corresponds to C–H stretching vibration modes of the hydrocarbon chains.

The FTIR spectra of *C. crispus* show two bands at 1650 and 1540 cm^{-1} (Fig. 4*a*). These bands are characteristic of

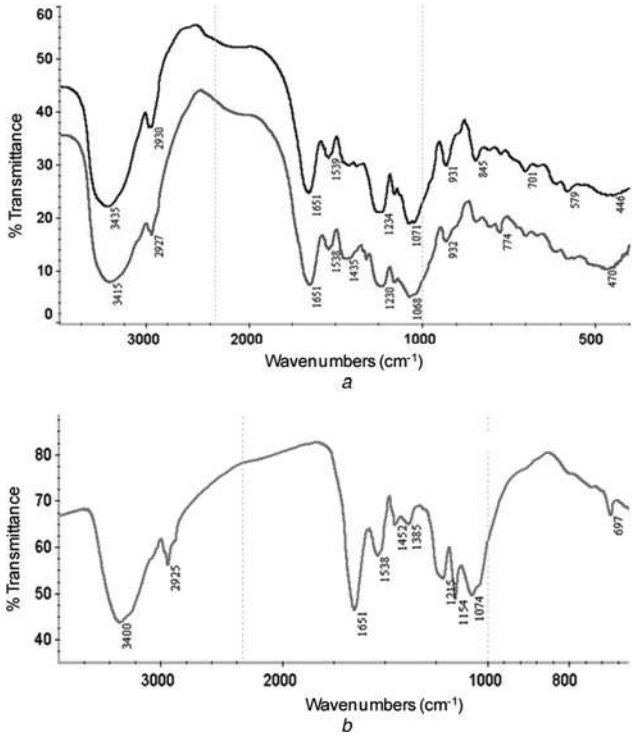

Fig. 4 *Functional groups involved in the biosynthesis of gold nanoparticles*

a FTIR spectra of *C. crispus* before the reaction (red) and *C. crispus* after the reduction (blue)
b FTIR spectrum of gold nanoparticles synthesised with *C. crispus*

amide I and II, respectively. Moreover, two intensive bands appear at 2300 and 1068 cm^{-1}. These bands could correspond to C–O–C and C = S stretching vibrations of thiocarbonyl derivates. The particles would be stabilised in solution by proteins and the xanthates of the seaweed.

FTIR analysis of gold nanoparticles (Fig. 4*b*) shows the presence of two bands at 1651 and 1538 cm^{-1} corresponding to amide I and II bands, respectively. In addition, the band at 1452 cm^{-1} is assigned to the methylene scissoring vibrations of proteins. The surface-bound is established through free amine groups or cysteine residues in the proteins [29, 30]. The other three intense bands at 1215, 1154 and 1457 cm^{-1} can be related to COC antisymmetric stretching, COC symmetric stretching and C = S stretching, which are characteristic of xanthates. *C. crispus* is rich in sulphur, which probably binds gold and can act as capping and stabilising agent of nanoparticles.

Use of green alga *Spirogira insignis: Spirogyra* is a genus of filamentous green algae and it is a member of the order *Zygnematales*. *Spyrogira* is named for the helical or spiral arrangement of the chloroplasts and is very common in relatively clean eutrophic water, developing slimy filamentous green masses. *S. insignis* is not a marine alga and this is a very interesting point for the research because it could be used for the synthesis not only of gold nanoparticles, but also of silver nanoparticles avoiding the silver chloride precipitation, which is signalled by greyish or purplish colouration in some samples.

3.1.4 Biosynthesis of gold nanoparticles: The biosynthesis of gold nanoparticles using *S. insignis* was obtained by addition of the biomass to different $HAuCl_4$

doi: 10.1049/iet-nbt.2012.0041

solutions with pH values from 2 to 10. The colour changed from pale yellow to pink or dark blue which is an indication of the formation of gold nanoparticles. The colour of the solutions and its intensity depended on the pH and the time of exposure (Fig. 5). The bluish solutions corresponded to the early stage of formation and related to aggregates of spherical nanoparticles or anisotropic nanostructures. The morphology of these nanoparticles was observed by TEM at different pH values. In all the cases, it was observed the agglomeration of small nanoparticles forming aggregates with several shapes at the beginning of the reduction process, even obtaining wire-like nanostructures (Fig. 6). These results correspond to a broad band in the UV–vis spectra (not shown), which is characteristic of the overlapping of the different absorptions at relevant wavelengths because of different sizes of the agglomerations.

The higher concentration of gold nanoparticles was reached after 2 h in contact with the green alga *S. insignis* at basic pH (Fig. 7*a*). The EDS spectrum of the nanoparticles (Fig. 7*b*) obtained by the treatment of $HAuCl_4$ aqueous solutions with the green alga confirmed the gold nature of the particles. Copper signals are because of copper grids.

After 2 h of reaction, we found that the intensity of the colour in the solutions and the absorbance of the bands measured with UV–vis spectroscopy decreased and the amount of nanoparticles observed by TEM was low. At low pH values, cell wall functional groups become highly protonated, resulting in an overall positive charge that attract electrostatically negatively. Kuyucak and Volesky [31] have suggested that the following reaction occurs

$$AuCl_4^- + 3R - OH \rightarrow Au^0 + 3R = O + 3H^+ + 4Cl^- \quad (1)$$

Equation (1) indicates that gold reduction is accompanied by the oxidation of hydroxyl to carbonyl groups present in the green alga and could participate in the gold recovery.

3.1.5 Biosynthesis of silver nanoparticles: Silver nanoparticles were biosynthesised using the green alga *S. insignis* by addition of the biomass to different $AgNO_3$ solutions with pH values from 4 to 10. The experiments were carried out avoiding the light. The colour changed to brownish and this change of colour indicated the reduction of the silver ions and the formation of the nanoparticles.

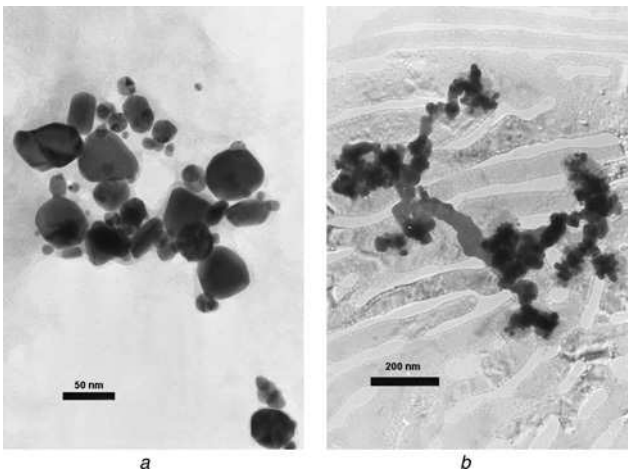

Fig. 6 *TEM images of gold nanostructures synthesised after 15 min of reaction using S. insignis at different initial pH values*
a Acidic pH
b Basic pH

It was observed that the efficiency of the silver nanoparticles formation at acidic pH was very low. Thus, the study and characterisation of the nanoparticles was performed at pH 6 and 10. At these pH values, a characteristic SPR band appeared after reaction of $AgNO_3$ with the green alga, which was centred at 460 nm. In addition, the UV–vis spectra showed other band at higher wavelength because of the agglomeration of the nanoparticles.

The yield of silver nanoparticle formation was also analysed by FAAS and the results showed an efficiency of 30% at low pH after 4 h and 60% at basic pH after only 1 h. These results could be explained by the competition between H^+ and metallic cations at acid pH. Furthermore, when the pH was increased, the time taken in the synthesis was reduced and the yield increased because ions OH^-

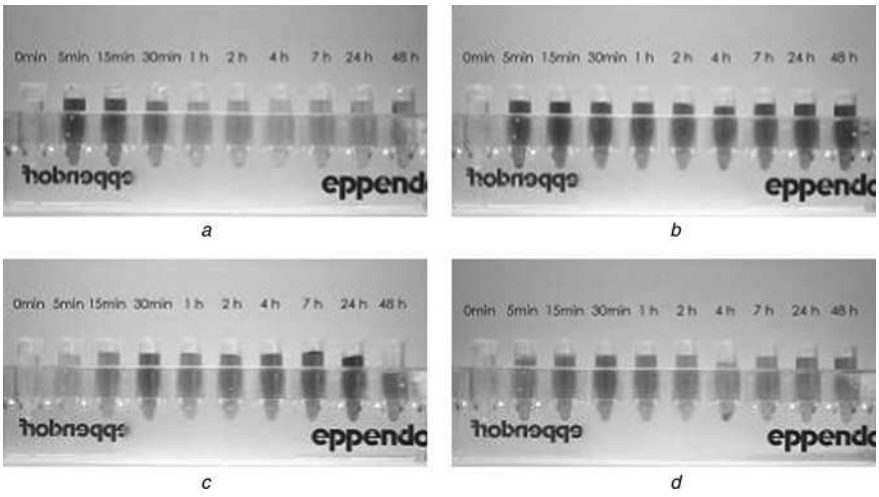

Fig. 5 *Colour changes of gold nanoparticle solutions at different pH values*
a pH 2
b pH 4
c pH 7
d pH 10

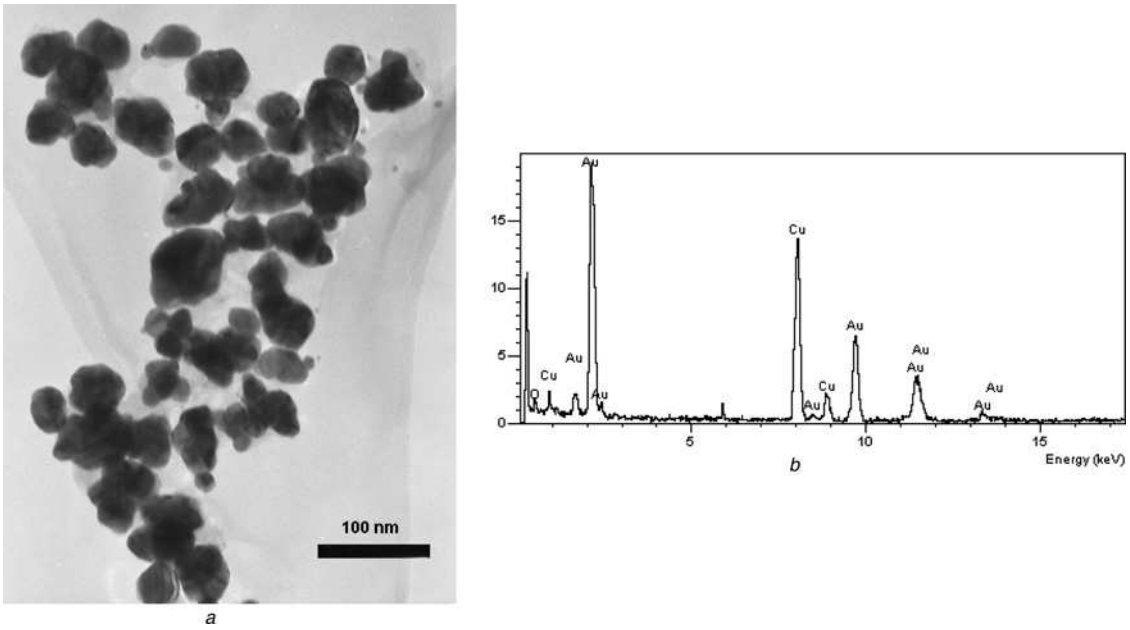

Fig. 7 *Biosynthesis of gold nanoparticle*

a TEM images of gold nanostructures synthesised after 2 h of reaction using *S. insignis* at different basic pH
b EDS of gold nanoparticles synthesised using *S. insignis*

agglomerated silver nanoparticles and their stability was enhanced [32].

TEM observations confirmed the presence of nanoparticle agglomerations in the solution (Fig. 8*a*). In case of silver nanoparticles, the shape was not well defined and the particles formed aggregates. The nanoparticles obtained were spheres and the diameter was approximately 30 nm. After more than 2 h of reaction, few nanoparticles were observed in the samples. EDS spectrum (Fig. 8*b*) evidenced the nature of the silver nanoparticles synthesised by reduction of $AgNO_3$ using the green alga.

The biomass after reaction was examined by SEM to confirm the biosorption mechanism (Fig. 9*a*). Silver particles were microprecipitated on the surface of the alga, especially at low pH. These precipitates were formed in a second stagethat was characterised by a decrease of silver ion concentration in solution and the decrease of colour in the solutions after 2 h. The brighter areas of the backscattered electron image correspond to metallic silver (Fig. 9*b*), as identified by EDS analysis, giving an evidence of the silver presence on the biomass.

3.1.6 Functional groups involved in the biosynthesis of nanoparticles:

The aim of the determination of the biomolecules involved in the reduction and formation of nanoparticles was studied by FTIR analysis of the biomass

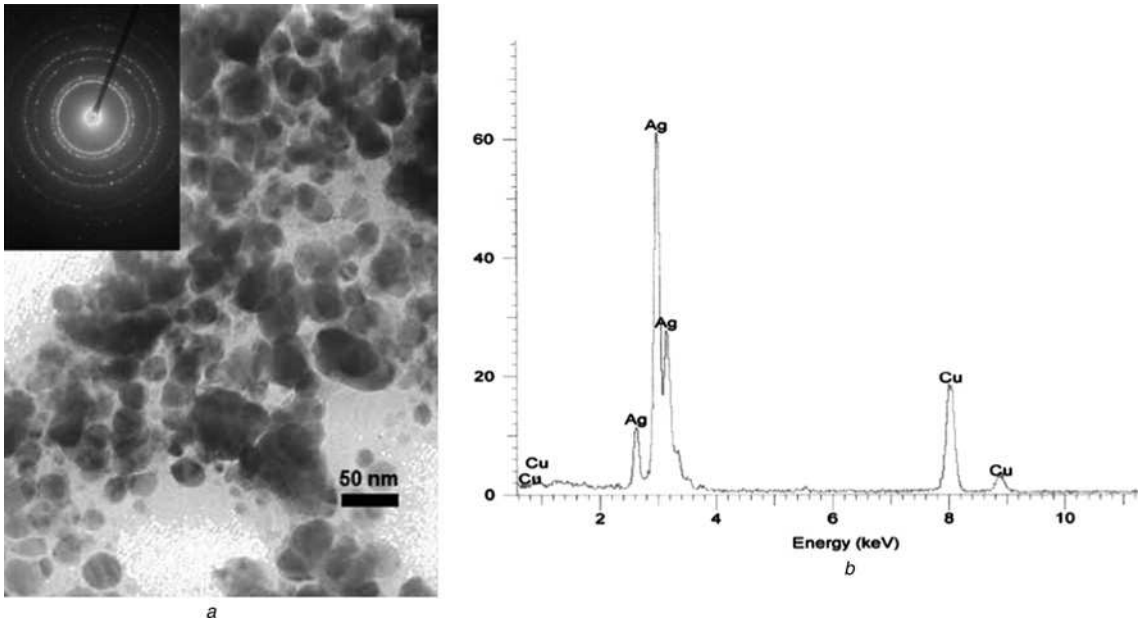

Fig. 8 *TEM observations confirmed the presence of nanoparticle agglomerations in the solution*

a TEM image of silver nanostructures synthesised after 2 h of reaction using *S. insignis*. The inset shows the electron diffraction pattern of silver nanoparticles
b EDS of silver nanoparticles synthesised using *S. insignis*

doi: 10.1049/iet-nbt.2012.0041

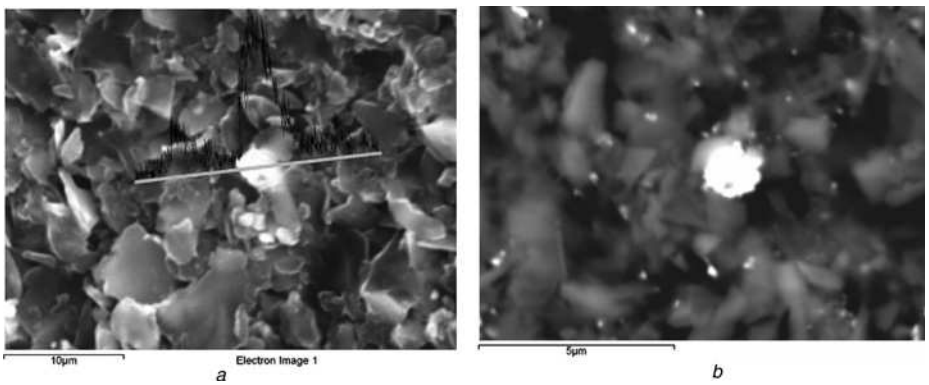

Fig. 9 *Biomass after reaction was examined by SEM to confirm the biosorption mechanism*

a SEM image of *S. insignis* after reaction and silver analysis
b Backscattered electron SEM micrograph of silver microparticles biosorbed onto the green alga

and of the nanoparticles (Fig. 10). FTIR analysis of the biomass (Fig. 10*a*) showed an intense broad band at a wavelength of 3369 cm^{-1} corresponding to the O–H stretching vibration modes of hydroxyl functional group in alcohols and N–H stretching vibrations in amides and amines. Furthermore, the absorption peak at 2926 cm^{-1} corresponds to C–H stretching vibration modes of the hydrocarbon chains. The FTIR spectrum of *S. insignis* also shows two bands at 1655 and 1540 cm^{-1}, which are characteristic of amide I and amide II, respectively. The first band presented a shoulder at higher wavelength overlapping the band corresponding to ketones and aldehydes. Moreover, the bands at 1369 cm^{-1} could be related to C–N stretching vibrations and the band at 1034 cm^{-1} to C–O stretching vibrations in polyalcohols.

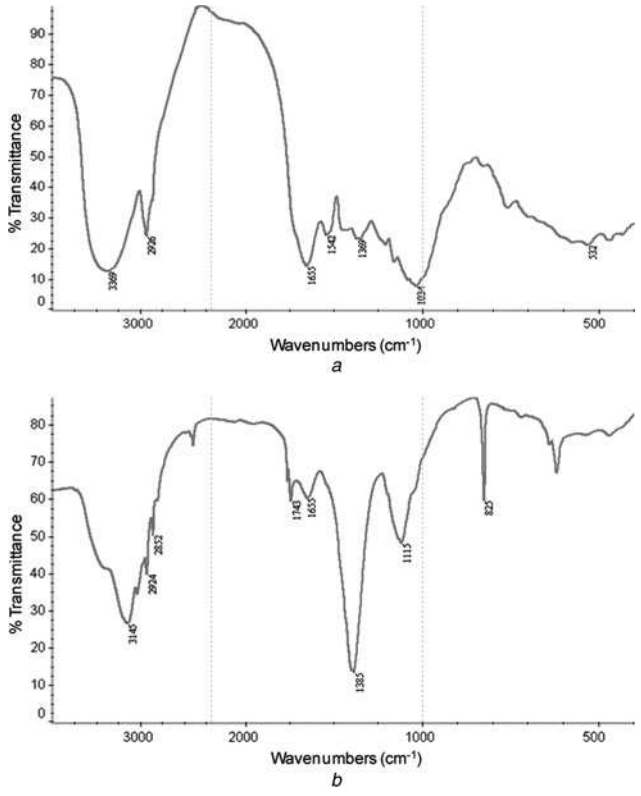

Fig. 10 *FTIR spectrum*

a Spirogyra insignis
b Silver nanoparticles synthesised with the green alga

The FTIR spectrum of the silver nanoparticles produced using *Spyrogira* (Fig. 10*b*) shows the presence of the methylene symmetric and antisymmetric stretching vibrations close to 2850 and 2920 cm^{-1}, respectively. The strong absorption peak at 3145 cm^{-1} corresponds to the stretching of the N–H bond of amino groups. The carbonyl groups from the aldehydes and ketones (1743 cm^{-1}) and amino acid residues (1655 cm^{-1}) have strong ability to bind silver and could stabilise nanoparticles in solution. The absorbance bands observed in the region of 1000–500 cm^{-1} correspond to alkenes and aromatic compounds. The most prominent vibrational mode observed at 1385 cm^{-1} in silver nanoparticles may be because of CN stretching mode (*N* from $AgNO_3$).

As dead biomass is used in the reduction reaction, metabolic processes are not involved in the nanoparticle formation. It is known that the outer cell wall of *Spyrogira* is composed of pectin that dissolves in water. Pectins are polysaccharides rich in galacturonic acid. The huge amount of hydroxyl groups in the cell wall could act as reductor of silver salt forming, in consequence, ketone groups. Unlikely, galacturonic acid is an acid sugar containing an aldehyde group and a carboxylic acid group. These deprotonated groups could attract metallic cations acting as centres of sorption.

4 Conclusions

In this work, algae are proposed for the biosynthesis of gold and silver nanoparticles as an efficient, eco-friendly and simple process. The gold nanoparticle size and shape could be directly controlled by the initial pH value of the solution, especially in case of the red seaweed *C. crispus*. In addition, the biosynthesis of gold and silver nanoparticles was also attained with the green alga *S. insignis* under the optimal conditions of synthesis including the possibility of metal recovery by sorption on the biomass surface. This is a preliminary study of the biological mechanism of nanoparticle biosynthesis and a first step in controlling the size of nanoparticles.

5 Acknowledgments

The authors acknowledge Juan Luis Bardonado from Centro de Microscopía Electrónica 'Luis Bru' and José E. Fernández from C.A.I. Espectroscopía Unidad Infrarrojo-Raman-Correlador of Complutense University of Madrid for their

technical assistance. We also thank the Spanish Ministry of Science and Innovation for funding this work.

6 References

1 Son, Y., Yeo, J., Moon, H., *et al*.: 'Nanoscale electronics: digital fabrication by direct femtosecond laser processing of metal nanoparticles', *Adv. Mater.*, 2011, **23**, (28), pp. 3176–3181

2 Cao, A., Lu, R., Veser, G.: 'Stabilizing metal nanoparticles for heterogeneous catalysis', *Phys. Chem. Chem. Phys.*, 2010, **12**, pp. 13499–13510

3 Cheng, Y., Samia, C.A., Meyers, J.D., Panagopoulos, I., Fei, B., Burda, C.: 'Highly efficient drug delivery with gold nanoparticle vectors for in vivo photodynamic therapy of cancer', *J. Am. Chem. Soc.*, 2008, **130**, (32), pp. 10643–10647

4 Vilela, D., González, M.C., Escarpa, A.: 'Sensing colorimetric approaches based on gold and silver nanoparticles aggregation: chemical creativity behind the assay. A review', *Anal. Chim. Acta*, 2012, **751**, pp. 24–43

5 Gao, C., Zhang, Q., Lu, Z., Yin, Y.: 'Templated synthesis of metal nanorods in silica nanotubes', *J. Am. Chem. Soc.*, 2011, **133**, (49), pp. 19706–19709

6 Weinberger, C.R., Cai, W.: 'Plasticity of metal nanowires', *J. Mater. Chem.*, 2012, **22**, pp. 3277–3292

7 Yuan, Q., Zhou, Z., Zhuang, J., Wang, X.: 'Pd–Pt random alloy nanocubes with tunable compositions and their enhanced electrocatalytic activities', *Chem. Commun.*, 2010, **46**, pp. 1491–1493

8 Chu, S., Ren, J., Yan, D., Huang, J., Liu, J.: 'Noble metal nanodisks epitaxially formed on ZnO nanorods and their effect on photoluminescence', *Appl. Phys. Lett.*, 2012, **101**, pp. 043122–6

9 Stephen, J.R., Macnaughton, S.J.: 'Developments in terrestrial bacterial remediation of metals', *Curr. Opin. Biotechnol.*, 1999, **10**, pp. 230–233

10 Mehra, R.K., Winge, D.R.: 'Metal ion resistance in fungi: molecular mechanisms and their regulated expression', *J. Cell. Biochem.*, 1991, **45**, pp. 30–40

11 Southam, G., Beveridge, T.J.: 'The *in vitro* formation of placer gold by bacteria', *Geochim. Cosmochim. Acta*, 1994, **58**, pp. 4527–4530

12 Beveridge, T.J., Murray, R.G.E.: 'Sites of metal deposition in the cell wall of *Bacillus subtilis*', *J. Bacteriol.*, 1980, **141**, (2), pp. 876–887

13 Sastry, M., Ahmad, A., Khan, M.I., Kumar, R.:. 'Microbial nanoparticle production', in: Niemeyer, C.M., Mirkin, C.A. (Eds.): 'Nanotechnology' (Wiley-VCH, 2004)

14 Narayanan, K.B., Sakthivel, N.: 'Biological synthesis of metal nanoparticles by microbes', *Adv. Colloid Interface Sci.*, 2010, **156**, pp. 1–13

15 Narayanan, K.B., Sakthivel, N.: 'Green synthesis of biogenic metal nanoparticles by terrestrial and aquatic phototrophic and heterotrophic eukaryotes and biocompatible agents', *Adv. Colloid Interface Sci.*, 2011, **169**, pp. 59–79

16 Luangpipat, T., Beattie, I.R., Chisti, Y., Haverkamp, R.G.: 'Gold nanoparticles produced in a microalga', *J. Nanoparticle Res.*, 2011, **13**, pp. 6439–6445

17 Govindaraju, K., Kiruthiga, V., Kumar, V.G., Singaravelu, G.: 'Extracellular synthesis of silver nanoparticles by a marine alga, *Sargassum wightii Grevilli* and their antibacterial effects', *J. Nanosci. Nanotechnol.*, 2009, **9**, (9), pp. 5497–501

18 Singaravelu, G., Arockiamary, J.S., Kumar, V.G., Govindaraju, K.: 'A novel extracellular synthesis of monodisperse gold nanoparticles using marine alga, *Sargassum wightii* Greville', *Colloids Surf. B, Biointerfaces*, 2007, **57**, (1), pp. 97–101

19 Rajasulochana, P., Dhamotharan, R., Murugakoothan, P., Murugesan, S., Krishnamoorthy, P.: 'Biosynthesis and characterization of gold nanoparticles using the alga *Kappaphycus alvarezii*', *Int. J. Nanosci.*, 2010, **9**, pp. 511–516

20 Senapati, S., Syed, A., Moeez, S., Kumar, A., Ahmad, A.: 'Intracellular synthesis of gold nanoparticles using alga *Tetraselmis kochinensis*', *Mater. Lett.*, 2012, **79**, pp. 116–118

21 Mata, Y.N., Blázquez, M.L., Ballester, A., González, F., Muñoz, J.A.: 'Gold biosorption and bioreduction with brown alga Fucus vesiculosus', *J. Hazardous Mater.*, 2009, **166**, pp. 612–618

22 Gericke, M., Pinches, A.: 'Biological synthesis of metal nanoparticles', *Hydrometallurgy*, 2006a, **83**, pp. 132–140

23 Gericke, M., Pinches, A.: 'Microbial production of gold nanoparticles', *Gold Bull.*, 2006*b*, **39**, pp. 22–28

24 Castro, L., Blázquez, M.L., Muñoz, J.A., Gonzalez, F., Garcia-Balboa, C., Ballester, A.: 'Biosynthesis of gold nanowires using sugar beet pulp', *Process Biochem.*, 2011, **46**, (5), pp. 1076–1082

25 Burdin, K.S., Bird, K.T.: 'Heavy metal accumulation by carrageenan and agar producing algae', *Botanica Marina*, 1994, **37**, pp. 467–470

26 Schwarzberg, A.M., Grant, C.D., van Buuren, T., Zhang, J.Z.: 'Reduction of $HAuCl_4$ by Na_2S revisited: the case for Au nanoparticle aggregates and against Au_2S/Au core/shell particles', *J. Phys. Chem. C*, 2007, **111**, pp. 8892–8901

27 Kelly, K.L., Coronado, E., Zhao, L.L., Schatz, G.C.: 'The optical properties of metal nanoparticles: the influence of size, shape, and dielectric environment', *J. Phys. Chem. B*, 2003, **107**, pp. 668–677

28 Grzelczak, M., Pérez-Juste, J., Mulvaney, P., Liz-Marzán, L.M.: 'Shape control in gold nanoparticle synthesis', *Chem. Soc. Rev.*, 2008, **37**, pp. 1783–1791

29 Binupriya, A.R., Sathishkumar, M., Vijayaraghavan, K., Yun, S.I.: 'Bioreduction of trivalent aurum to nano-crystalline gold particles by active and inactive cells and cell-free extract of Aspergillus oryzae var Viridis', *J. Hazardous Mater.*, 2010, **177**, pp. 539–545

30 Dubey, S.P., Lahtinen, M., Sillanpää, M.: 'Tansy fruit mediated greener synthesis of silver and gold nanoparticles', *Process Biochem.*, 2010, **45**, pp. 1065–1071

31 Kuyucak, N., Volesky, B.: 'Accumulation of gold by algal biosorbent', *Biorecovery*, 1989, **1**, pp. 189–204

32 Sanghi, R., Verma, P.: 'Biomimetic synthesis and characterisation of protein capped silver nanoparticles', *Bioresour. Technol.*, 2009, **100**, pp. 501–504